



Connectivity dynamics in vehicular freeway scenarios

Ossama Hamouda, Mohamed Kaâniche, Erling Moller Matthiesen, Jakob Gulddahl Rasmussen, Hans-Peter Schwefel

► To cite this version:

Ossama Hamouda, Mohamed Kaâniche, Erling Moller Matthiesen, Jakob Gulddahl Rasmussen, Hans-Peter Schwefel. Connectivity dynamics in vehicular freeway scenarios. Global Information Infrastructure Symposium (GIIS '09), Jun 2009, Hammamet, Tunisia. pp.1-8, 10.1109/GIIS.2009.5307090 . hal-00851876

HAL Id: hal-00851876

<https://hal.science/hal-00851876>

Submitted on 23 Aug 2013

HAL is a multi-disciplinary open access archive for the deposit and dissemination of scientific research documents, whether they are published or not. The documents may come from teaching and research institutions in France or abroad, or from public or private research centers.

L'archive ouverte pluridisciplinaire **HAL**, est destinée au dépôt et à la diffusion de documents scientifiques de niveau recherche, publiés ou non, émanant des établissements d'enseignement et de recherche français ou étrangers, des laboratoires publics ou privés.

Connectivity dynamics in vehicular freeway scenarios

Ossama Hamouda^{1,2}, Mohamed Kaâniche^{1,2}, Erling Matthiesen Møller³,
Jakob Gulddahl Rasmussen³, Hans-Peter Schwefel^{3,4}

¹ CNRS; LAAS; 7, avenue du Colonel Roche, F-31077 Toulouse, France

² Université de Toulouse; UPS, INSA, INP, ISAE; LAAS-CNRS : Toulouse, France
{ossama.hamouda, mohamed.kaaniche}@laas.fr

³ CTIF, Aalborg University, Niels Jernes Vej 12/A5-212, 9220 Aalborg-Øst, Denmark
evm@es.aau.dk, jgr@math.aau.dk

⁴ Forschungszentrum Telekommunikation Wien - FTW, Donau - City Straße 1, 1220 Vienna, Austria
hps@es.aau.dk

Abstract—Vehicular ad-hoc networks have received increasing interest in the last years for their potential to support a variety of services and applications in order to improve driving safety or traffic efficiency and to provide information and entertainment to the users. This paper focuses on the analysis of some connectivity characteristics in dynamic vehicular communication scenarios, that are important for the design and the performance and dependability assessment of such applications. In particular, we focus on the process describing the occurrence of encounters between cars in single and multi-hop scenarios. Using analytical proofs and simulation experiments, it is shown that under some key assumptions on the movements and the placement of the cars, this process can be approximated as a stationary or a nonhomogeneous *Poisson* process. Results are also provided concerning the duration of connections in the ad-hoc domain.

Keywords: ad-hoc networks, vehicular networks, connectivity dynamics

1. INTRODUCTION

Vehicular communication scenarios are characterized by high dynamicity and challenging propagation environments, while at the same time the communicating applications are frequently having safety-critical nature and hence are subject to high availability and reliability requirements [1]. In order to provide and analyze the quality of service required by such applications, it is important to characterize the connectivity between the highly mobile nodes. For static snapshots of certain mobility models in vehicular freeway scenarios, Reference [2] develops solutions of stochastic models and discusses numerical results. Certain application types and support functions, such as the Distributed black-box and dynamic data and service replication in the vehicular domain [3], can benefit from dynamic changes of the connectivity set.

This paper focuses on the analysis of the stochastic process describing the moments in time at which a particular vehicle enters a new k -hop connectivity relation with another vehicle. Due to requirements of route stability and low end-to-end delay, low values of k are of particular interest. Hence, large parts of the paper focus on direct neighborhood relations ($k = 1$). Link-layer connectivity can thereby be established as soon as the distance between two vehicles is below a certain value R , called the communication radius [4], see Section 3 for more details.

Section 4 proves that under certain conditions, most notably independent movement of vehicles at different but constant speed and initial spatial *Poisson* placement of vehicles on a 1-dimensional space, the process of meeting new direct neighbors is a *Poisson* process, whose rate, α , can be expressed as the product of the vehicle density and the expected value of the absolute relative speed of the other vehicles. Section 5 discusses the consequences of the proven result for single straight freeways with multiple lanes, in particular characterizing the impact of changing communication radius R . Deviations from the *Poisson* property and the obtained relation for the *Poisson* rate α are then investigated for increasingly complex mobility models that deviate from the original assumptions of the proof in Section 4. In Section 3, independent movement of vehicles on a finite long stretch of freeway are investigated, while in Section 6, traces from a more complex mobility model that includes dependencies between individual vehicles and varying speeds are investigated.

2. RELATED WORK

Much of the existing work on connectivity analysis in ad-hoc networks focuses on static snapshots of the node placement: [5] analyses different connectivity metrics under the assumption that the node placement can be described by a spatial renewal process. This setting is generalized in [6] to cases of spatial correlation described by Markovian Arrival Processes [2]. The metrics thereby include distribution and moments for the number of direct neighbors (single-hop) and for the number of reachable nodes via multi-hop connections. Furthermore, spatial distances and hop-count distributions are characterized and analyzed via numerical results. In comparison to this existing work, this paper focuses on models that describe the dynamics of the connectivity, specifically the stochastic processes that describe the intervals between time instances in which new nodes get into single or multi-hop connectivity range.

This problem has been seldom investigated in the context of vehicular ad-hoc networks. It is noteworthy that some recent work has been done in this direction in the context of encounter-based protocols. We can cite for example [7] which presents an analytical methodology for calculating a number of encounter-related statistics including inter-encounter times and

encounter duration considering popular epoch-based mobility models such as the Random Waypoint mobility model, and Random Direction mobility model.

3. FREEWAY MOBILITY AND CONNECTIVITY MODEL

Many of the future *Telematics Applications* [8, 9] are particularly relevant in vehicular freeway scenarios, as the high speeds together with the rather structured geographical movements make safety applications relevant and feasible. Figure 1 shows an abstraction of such a vehicular freeway scenario, used in our context to analyze and estimate some connectivity characteristics between the mobile nodes (*i.e.*, “vehicles”). We consider a long straight piece of freeway with movements in two directions. In the example of Figure 1, all cars on the upper half of the freeway (with width W) move to the right, while cars on the lower half move into the opposite direction. The considered piece of freeway has a finite length of $L \gg W$. In order to avoid edge effects, we assume in simulations that cars that leave on one side enter at the corresponding point on the other side, *i.e.*, the long piece of road can be seen wrapped around a cylinder. The individual directions themselves may have multiple lanes, but as we in large parts of the paper assume that cars move independently of each other, the actual concept of lanes within the same direction is irrelevant. As a starting assumption, vehicles have a constant (absolute) speed v_i which is assumed to be *i.i.d.* with probability density function $f_{abs}(v)$.

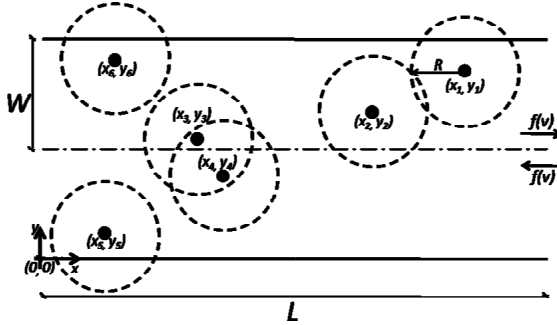


Figure 1: The mobility model scenarios

In order to focus on understanding the impact of the geographic mobility model, we adopt the approximation that two nodes can communicate on a direct link when their geographic Euclidean distance is less than a communication radius R , where R is a constant for all nodes regardless of speeds (so neglecting Doppler shifts). Hence, we assume a homogeneous communication technology and avoid having to describe detailed influence of the communication environment. In order to avoid technicalities in the derivations, we later on also utilize squared connectivity areas, *i.e.*, two cars can communicate if their distance with respect to the supremum-norm is less than R , *i.e.*, $\max\{x_1 - x_2, y_2 - y_1\} \leq R$.

In order to define metrics to characterize connectivity dynamics, we consider a reference vehicle located at position (x_b, y_b) . In this paper we analyze two metrics:

- The temporal *Node Encounter Process*, E , which describes the time instances at which other cars enter (single-hop or k -hop) connectivity to the reference car. For $k=1$, these moments correspond to new cars coming

into radio range R of the reference car. The mean time between such encounters is represented by α^{-1} and α is called the rate of the encounter process.

- The *duration of the Connectivity Periods*, which is the random variable describing the length of the time-interval starting when another node enters into k -hop connectivity range of the reference node and ending when this node leaves k -hop connectivity. The mean duration of the connectivity period is denoted by T .

In the following, we first prove that under certain assumptions, the nodes encounter process is a *Poisson* process with rate α and come up with a relation to calculate α . Then, we compare this result with simulations of more general mobility models as reflected by Figure 1, investigating first the case of independent movements of vehicles and then accounting for dependencies between movements of different vehicles.

4. PROOF OF POISSON ENCOUNTER PROCESS

In this section we show that under certain scenario assumptions, the encounter process is a *Poisson* process with rates α that can be calculated from the car density and the expected absolute value of the relative speed distribution.

Assuming a quadratic connectivity range for the mobility scenario with independent movements in Figure 1, the vertical dimension of the scenario is irrelevant and we can simplify the freeway model to a 1-dimensional movement scenario. We now assume that the road is infinitely long and the initial placement of the cars is a spatial *Poisson* process. We place the reference vehicle at position 0 at all times, and let the other vehicles, say x_i , move with constant velocities v_i drawn from a continuous distribution V with density f (*i.e.*, we consider their relative velocity to the reference vehicle). The following theorem then shows that the single-hop encounter process E of meeting new direct neighbors in this case is a *Poisson* process.

Theorem 1: Let X be a *Poisson* process with intensity $\rho(x)$ for $x \in \mathbb{R}$, and v_i be *i.i.d.* continuous random variables with density f . Then the encounter process E is a *Poisson* process with intensity

$$\alpha(t) = \int_0^\infty \rho(R - vt) f(v) v dv - \int_{-\infty}^0 \rho(-R - vt) f(v) v dv$$

provided α is locally integrable. In the case where X is stationary with intensity ρ , the encounter process E is also stationary and has intensity

$$\alpha = \rho E|V| \quad (1)$$

where V is a random variable with density f provided $E|V| < \infty$.

Proof: Let X_1 and X_2 denote the point processes of those $x_i \in X$ with $v_i > 0$ and $v_i < 0$, respectively. Since v_i are *i.i.d* and they are independent of X , X_1 and X_2 are independent thinning of X , so they are *Poisson* with intensities $p\rho(x)$ and $(1-p)\rho(x)$, where $p = P(v_i > 0)$ (see e.g. [10]).

Consider first X_1 . Since the vehicles in X_1 have a higher velocity than the vehicle at zero, these will get into communication range at position R . The time at which this occurs for a vehicle with position x_i at time zero is given by

$t_i = -(x_i - R)/v_i$; denote the process of these t_i by E_1 . Since v_i is distributed with density $f_i(x) = f(x)/p$ on $(0, \infty)$ (i.e., f restricted to the positive half-line), the conditional distribution of t_i given x_i has density

$$f_1\left(-\frac{x_i - R}{v_i}\right) \cdot \left|\frac{x_i - R}{v_i^2}\right|$$

By Proposition 3.9 in [10], E_1 is a *Poisson* process with intensity

$$\begin{aligned} \alpha_1(t_i) &= \int_R p\rho(x_i) f_1\left(-\frac{x_i - R}{v_i}\right) \cdot \left|\frac{x_i - R}{v_i^2}\right| dx_i \\ &= \int_0^\infty \rho(R - vt_i) f(v) v dv \end{aligned}$$

where the transformation $v = -(x_i - R)/t_i$ has been used.

Similarly it can be shown that E_2 , the process of t_i resulting from $x_i \in X_2$, is a *Poisson* process with intensity

$$\alpha_2(t_i) = \int_0^\infty \rho(-R - vt_i) f(v) (-v) dv$$

Since X_1 and X_2 are independent, E_1 and E_2 are also independent, so their superposition is a *Poisson* process with intensity $\alpha(t) = \alpha_1(t) + \alpha_2(t)$ (see e.g. [10]), from which the first assertion follows. The stationary case follows directly by letting ρ be constant in the expression for $\alpha(t)$.

5. SIMULATION OF INDEPENDENT MOVEMENTS SCENARIOS

The rigorously proven theorem in the previous section relies on three key assumptions: (1) infinite, 1-dimensional stretch of freeway, (2) initial *Poisson* placement of cars, (3) independent movements of cars over time at constant speed selected from some given distribution. In this section, we will check the sensitivity of the *Poisson* result towards slight deviations from Assumptions (1) and (2) by investigating slightly more complex freeway mobility scenarios as described in Section 3. The impact of mobility models deviating from Assumption (3) is investigated in Section 6.

Subsequently, we perform simulation experiments in order to compare with the *Poisson* result of the previous section and to validate to what extent Equation (1) provides a useful quantitative approximation even in more complex mobility models. We therefore consider the 2-dimensional spatial scenario described in Figure 1. Vehicles move in two different directions with the following example selection of a uniform speed distribution and uniform initial placement:

- Each vehicle has a constant speed selected at the beginning of the simulation uniformly distributed between v_{min} and v_{max} ;
- Each vehicle is assigned x coordinate between $(0, L)$ and y coordinate between $(0, 2W)$ according to a uniform distribution;
- The reference vehicle at the beginning of the simulation is assigned initial coordinates (x_l, y_l) and speed v_l .

Unless specified differently, we use the following set of default parameters: the freeway has a geometry of $L = 5000m$

and $W = 15m$; the car density is $\rho = 1car/100m$; the bounds for the uniform distribution for the initial speed are $v_{min} = 80km/h$ and $v_{max} = 130km/h$; the communication radius is $R = 25m$ and the initial placement of the reference car is $(x_l, y_l) = (2500m, 22.5m)$ with speed $v_l = 108km/h$. Note that for this set of default parameters, the communication range of the reference car covers the full width of the freeway in both driving directions. Also, the expected absolute value of the relative speed in comparison to the reference car results as $Ev_{rel,1} = 31.287 m/sec$.

The geographic movement of the cars is simulated considering fixed time steps of granularity $0.1sec$. Time steps at which k -hop connectivity relations to the reference car are established newly or vanishing are recorded. The results from the simulation model are used to investigate the distribution of the inter-encounter times. In the second part of this section, we analyze the impact of the communication range on the encounter process rate both by detailing Equation (1) and by simulations. Finally, we analyze the distribution and expected value of the connectivity periods. In most parts of the section, we focus on single-hop connectivity ($k=1$).

5.1. Marginal distribution of single-hop inter-encounter times

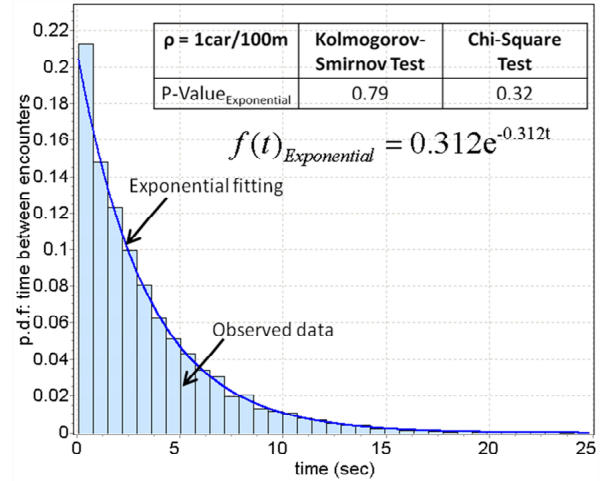


Figure 2: Empiric probability density function of the time between single-hop encounters for, car density $\rho = 1car/100m$: simulation results and comparison to an exponential distribution with its rate computed from Equation (1)

Figure 2 plots the empiric probability distribution function for the inter-encounter time in the single-hop case obtained from samples from 300 simulation runs, each entailing $5hrs$ simulated time (approximately 600 encounter samples in each run). Statistics for the times between encounters observed from the simulation show a *mean* = $3.34sec$ corresponding to a rate estimate $\hat{\alpha} = 0.29/sec$ and a variance of inter-encounter times = $10.38sec^2$. The encounter rate value that results from Equation (1) is $\alpha = 0.312/sec$, so rather close to the simulation estimate (see later for confidence intervals). Also, the empiric marginal distribution represents a close fit to the exponential distribution with rate $\alpha = 0.312/sec$. This is confirmed by applying Kolmogorov-Smirnov and χ^2 tests for exponential distribution. As shown in Figure 2, the P-Value for each of these tests is acceptable for confidence levels equal to 5%.

Note that the actual simulated mobility model deviates from the assumptions of the proof in: (1) the road length is finite; (2) the road width is not zero; however as cars keep their y-coordinate during the simulation runs and the communication range covers the full road width, there is no expected impact on the results; (3) the initial placement is using uniformly distributed coordinates, which however for large number of cars converges to a spatial *Poisson* distribution. With decreasing node density, the impact of (1) and (3) becomes stronger and deviations from the *Poisson* properties of the encounter process become more pronounced.

5.2. Impact of the communication radius R

Note that the encounter rate α as resulting from Equation (1) does not show a direct dependence on the communication radius R . However, if R is so small that it does not cover the full width of the freeway, there is an indirect dependence, as not all vehicles driving in the opposite direction can come into range, hence both the effective vehicle density ρ and also the expected value of the relative speed will depend on the communication radius in that case. In the following, we quantify such dependence for the example case of a uniform speed distribution. The calculation can be performed analogously for any speed distribution.

Let us consider the reference vehicle at position (x_l, y_l) shown in Figure 1. As mentioned in Section 3, each vehicle has a connectivity range R . Let us denote by P_1 the fraction of the upper lane (in which the reference vehicle is placed) that is covered by R . The upper lane is completely covered ($P_1 = 1$), when y_l satisfies the condition: $R \geq \max(2W - y_l, y_l - W)$. For other cases ($P_1 < 1$), two situations should be distinguished:

1) if the radio range R of the reference vehicle does not cross

$$\text{the other lane } (R < y_l - W), \quad P_1 = \frac{R + (2W - y_l)}{W}$$

2) otherwise, $P_1 = \frac{R + (y_l - W)}{W}$

Similarly let us define by P_2 the fraction of the lower lane covered by R . It can be shown that P_2 is obtained by:

$$P_2 = \min(1, \max(0, \frac{R + W - y_l}{W})).$$

As a consequence, the effective car density which only takes into account cars that can come into connectivity range is:

$$\rho(R) = \rho \frac{P_1 + P_2}{2} \quad (2)$$

Given that the absolute speed of the cars is distributed according to $f(v)$, we need to go through some technicalities in order to compute the expected relative speed, which we illustrate here for the case of the uniformly distributed speed.

Considering the case where $v_1 < \frac{v_{\max} - v_{\min}}{2}$, we need to distinguish the three following situations:

- Vehicles have a larger speed than the reference vehicle and are in the same lane where the reference vehicle is.

Let us denote by S_1 , the average relative speed corresponding to this case.

$$S_1 = \int_0^{v_{\max} - v_1} v \cdot f_1(v) \cdot dv \text{ where, } f_1(v) = \frac{P_1}{P_1 + P_2} f_{abs}(v)$$

- Vehicles have a smaller speed than the reference vehicle and are in the same lane where the reference vehicle is. Let us denote by S_2 , the average relative speed corresponding to this case.

$$S_2 = \int_0^{v_1 - v_{\min}} v \cdot f_1(v) \cdot dv$$

- Vehicles are in the other lane where the reference vehicle is. Let us denote by S_3 , the average relative speed corresponding to this case.

$$S_3 = \int_{v_{\min} + v_1}^{v_{\max} + v_1} v \cdot f_2(v) \cdot dv \text{ where, } f_2(v) = \frac{P_2}{P_1 + P_2} f_{abs}(v)$$

Taking into account the $v_1 < \frac{v_{\max} - v_{\min}}{2}$ and by combining the three averages S_1 , S_2 , and S_3 together, the average relative speed is obtained as follows:

$$E|V| = \int_0^{v_1 - v_{\min}} f_1(v) \cdot v \cdot dv + \int_{v_1 - v_{\min}}^{v_{\min} + v_1} f_1(v) \cdot v \cdot dv + \int_{v_{\min} + v_1}^{v_{\max} - v_1} v \cdot dv + \int_{v_{\max} - v_1}^{v_{\max} + v_1} f_2(v) \cdot v \cdot dv$$

Considering the case of uniform distributed speeds $f(v) = \frac{1}{v_{\max} - v_{\min}}$ for $v_{\min} \leq v \leq v_{\max}$, the average relative speed is given by:

$$E|V| = - \frac{(v_{\max}^2 + 2v_1(v_{\max} - v_{\min}) - v_{\min}^2)P_2 + ((v_1 - v_{\min})^2 + (v_1 - v_{\max})^2)P_1}{2(v_{\min} - v_{\max})(P_1 + P_2)}$$

The same procedure can be applied for the other case where

$$v_1 \geq \frac{v_{\max} - v_{\min}}{2}$$

Finally we get: $\alpha(R) = \rho(R) \cdot E|V|$ from Equation (1).

For the remaining of this section, we will consider the case where $v_1 < \frac{v_{\max} - v_{\min}}{2}$.

Figure 3 plots the resulting $\alpha(R)$ from this calculation for different values of R and compares it to the estimated encounter rate from our simulations. Despite the small deviations of the mobility model from the underlying assumptions of Equation (1), calculated values are always within the 95% confidence intervals of the simulation estimates. We can note that for radio ranges with $P_2 = 0$ the encounter rate is increasing slowly then dramatically increases, during the period $P_2 > 0$, until it reaches a saturated state when P_1 and P_2 are equal to one.

When extending our simulation analysis to also count 2-hop connectivity via relaying nodes, the empiric distribution of the time between encountering new (single-hop or 2-hop) neighbors is shown in Figure 4. There is no theoretically proven result for this connectivity case, but as the *Poisson* result in Section 4 is actually insensitive to the communication range (except for the artifacts for small R discussed in the previous section), there is some hope that a *Poisson* approximation may still be reasonably close. Figure 4 confirms visually the appropriateness of an exponential approximation for the considered scenario.

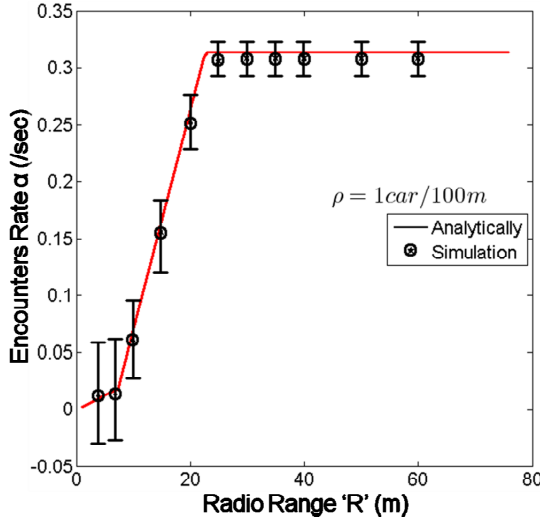


Figure 3: The impact of the Radio Range on the encounter rate α

5.3. Multi-hop connectivity dynamics

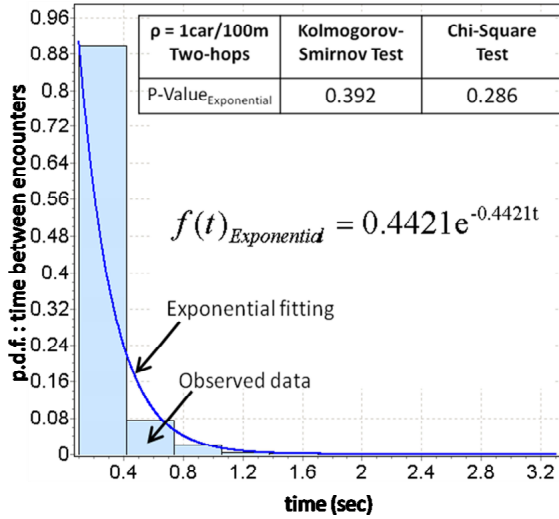


Figure 4: p.d.f of time between encounters: simulation results and curve fitting, $\rho = 1\text{car}/100\text{m}$ and 2-hops connectivity

The simulation estimate of the encounter rate from the simulation data is $\hat{\alpha} = 0.44/\text{sec}$. The increased encounter rate for the 2-hop case results from the fact that: (a) obviously, any car can only communicate with the reference car if its distance is below $2R$; (b) while being in that distance range however, a car can get into and out of connectivity to the reference car multiple times caused by relay nodes gaining or losing single-hop connectivity. It is noteworthy that, for three and four hops connectivity scenarios (not shown here), the exponential distribution is also a good approximation in the considered cases, which led to estimated rates $\alpha(k=3)=0.458/\text{sec}$ and $\alpha(k=4)=0.552/\text{sec}$, respectively. With the analogous arguments as for the 2-hop case, the meet rate increases slightly with increasing number of hops. Analytic derivations for this case comparable to Section 4 are beyond the scope of this paper.

5.4. Connectivity duration characterization

For many application cases, not only the process of meeting new nodes in connectivity range is relevant, but also the duration of the connectivity period. For the single-hop connectivity case with squared connectivity range (*i.e.*, whenever the distance of 2 nodes with respect to the supremum-norm is smaller than R , the two nodes can communicate), we again utilize the mobility model of the previous sections. Under these assumptions, the random variable T describing the connectivity duration results from: $T = 2R/|V_{\text{rel}}|$. Hence, when $f(v)$ is the density function of the absolute value of the relative speed, the connectivity duration has density:

$$g(t) = f(2R/t) \frac{2R}{t^2} \quad (3)$$

For circular connectivity range, the calculation of the density becomes slightly more complicated as the distribution of the vertical distance between the nodes has to be taken into account. We skip the technical details here and focus on squared connectivity ranges.

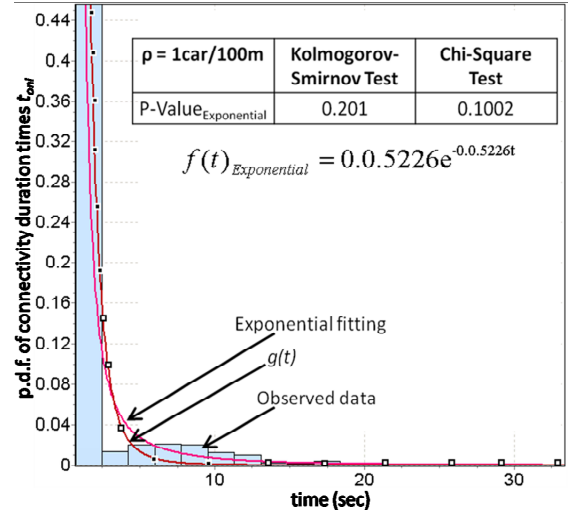


Figure 5: Simulation results: p.d.f of connectivity duration

Figure 5 plots the empiric probability density function obtained from the same simulation experiments as used for the encounter process; the histogram is based on 180000 samples. The figure also plots the expected probability density function resulting from Equation (3), where $f(v)$ is the resulting density of the absolute value of the relative speed as computed for the case of uniform distributed speeds in Section 5.2. Also shown in the figure is an exponential fitting of the empiric distribution. This exponential approximation may be useful when connectivity dynamics are reflected by Markov models in performance and dependability models, see *e.g.* [11]. The estimate of the expected value of the connectivity duration from the simulation data is 2.018sec , so the exponential fit has rate parameter $\hat{\beta} = \hat{T}^{-1} = 0.5226/\text{sec}$.

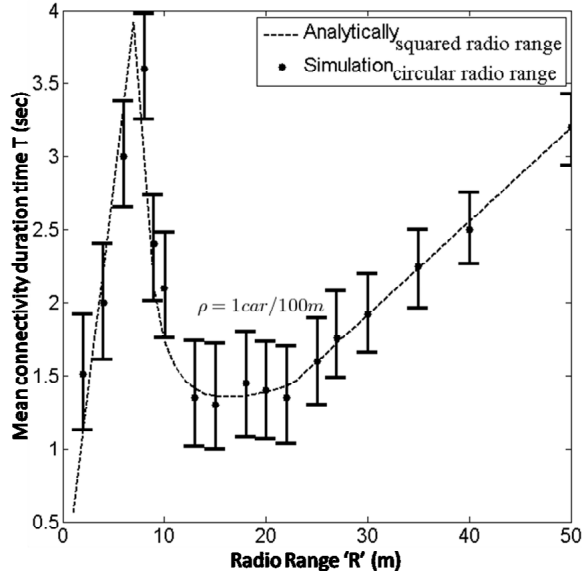


Figure 6: The impact of the Radio Range on the expected connectivity duration

As derived in Section 4, the expected value of the relative speed is a function of the connectivity radius R as long as $R < \max(y_l, 2W - y_l)$. The expected value of T can then be calculated as:

$$E(T) = \frac{2R}{E|V|} \quad (4)$$

where both the numerator and denominator depend on R .

Figure 6 shows the evolution of the mean connectivity duration time for different values of the communication range R . This figure also plots the estimated values from simulation experiments with the following parameters: $\rho = 1 \text{ car}/100\text{m}$, $v_{\min} = 80 \text{ km/hr}$, $v_{\max} = 130 \text{ km/hr}$, $v_l = 108 \text{ km/hr}$, $L = 5000\text{m}$, $W = 15\text{m}$, $(x_l, y_l) = (2500\text{m}, 22.5\text{m})$. The radio range in the simulation is of circular shape, which shows its impact only for small values of R . It can be observed that $E(T)$ first increases with the radio range R till the radio range covers the upper lane entirely, and decays subsequently (as vehicles from the lower lane with high relative speed contribute to the connectivity events). Starting from $(R = y_l)$, $E(T)$ starts to increase linearly with R .

6. MOBILITY WITH DEPENDENCIES BETWEEN VEHICLES

One of the key assumptions in the simulation models of the previous section was that the cars move independently of each other at fixed speed (though different between cars) and they do not change lanes. As we saw in the simulation results, we are in such settings close to the assumptions of the mathematical theorem in Section 4, and hence a Poisson process is a close approximation for the encounter process, even in multi-hop connectivity settings. We could also derive and analyze the distribution of the connectivity duration and the impact of the connectivity range on the expected value of both parameters.

In this section, we remove the assumption of independence between cars by utilizing publicly available mobility traces

that were produced by a more complex simulation model [12]. The traces describe a vehicular freeway scenario containing also two driving directions, where each direction has either two or three lanes. The dimensions of the freeway are 2.5m per lane and a 2m gap between the two sets of lanes. Each trace file contains 120 time steps of granularity 0.5s , which is coarser than in the earlier simulations.

As compared to the previous section, the car movement in these mobility traces now shows variable speeds, cars can get slowed down by slower cars in front of them, and they need to change lanes and speed up in order to pass by. Hence, these simulations show strong correlation between the trajectories of different cars (except for sparse car densities when there is little mutual obstruction). Speed values thereby are in the range of 57.6 km/h up to 197 km/h .

In contrast to the simulations in the previous section, the freeway is now not considered wrapped around a cylinder, but cars enter on one side and leave at the other end.

Figure 7 illustrates the changing speeds for a set of cars in one of the traces. Since the absolute speeds are varying, also the absolute value relative speed with respect to a reference car i , $v_{\text{rel},i}(t)$, is a function of t . Therefore the estimate of the expected value of this relative speed (averaging over the ensemble of cars $j \neq i$) is a function of time, illustrated for different reference cars in Figure 7. As a consequence of this mobility model, both the car density and also the expected value of the absolute value of the relative speed are time-dependent.

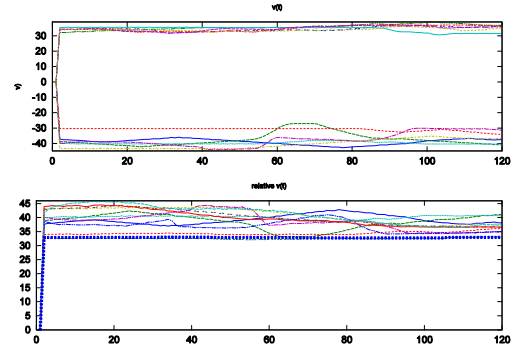


Figure 7: Vehicle speed and speed relative to the observed vehicle (unit: m/sec)

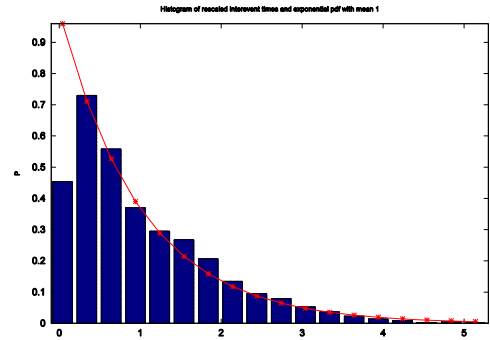


Figure 8: Histogram of the rescaled interevent times, and a pdf of an exponential distribution with $\text{mean}=1$

6.1 Connectivity duration characterization

As both the vehicle density and also the average relative speeds are time-dependent, we cannot apply the results and analysis approach of Sections 4 and 5 directly to this scenario. Instead, we investigate the following conjecture:

The process that vehicle i meets new direct neighbors can be approximated by an inhomogeneous Poisson process with rate $\alpha_i(t) = \rho(t)v_{ref,i}(t)$.

As cars enter and leave not exactly at the beginning and end of the freeway, we adopt the following approach to obtain $\rho(t)$ from the simulations: Let $d(t)$ be the distance between the last two cars at the beginning and end of the freeway stretch. $\rho(t) = N(t)/d(t)$ is then the number of cars on the freeway at time t divided by this spatial distance. The mean relative speed is determined by averaging over the cars that are on the freeway at time t , as illustrated in the lower part of Figure 7.

In the following, we observe the inter-encounter times in trace-driven simulations with these mobility traces for which we assume a connectivity range $R=100m$. To check visually whether the inter-encounter times can be approximated by a inhomogeneous *Poisson* process, we plot the empiric density of the re-scaled inter-encounter time, where we rescale by the rate $\alpha_i(t) = \rho(t)v_{ref,i}(t)$, and then compare to an exponential density with rate 1. This comparison is shown in Figure 8. Except for the very first bin of the histogram (corresponding to small re-scaled inter-encounter times), the exponential density shows an excellent match.

When comparing the empiric Cumulative Distribution Function (cdf) of the rescaled inter-encounter times with an exponential cdf of rate 1 ($F(t)=1-e^{-t}$), the deviations with respect to the number of small samples in Figure 8 will lead to some initial vertical offset in the cdfs, which will only gradually reduce. In order to quantify the deviation from the inhomogeneous *Poisson* assumption, we define as goodness-of-fit metric the re-scaled distances between the empiric cdf and the exponential cdf:

$$GOF = \frac{1}{C} \int_0^\infty \left| \hat{F}(t) - F_{exp}(t) \right| dt$$

where C is chosen to renormalize the value to the range between 0 and 1; 0 indicates an exact fit, while 1 represents the strongest deviation from the exponential distribution.

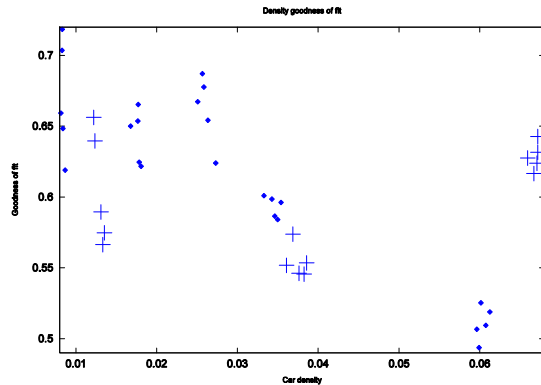


Figure 9: Scatter plot showing the goodness of fit against the car density. The scenarios that contain 3 lanes per freeway direction are marked as diamonds, 2-lane scenarios are shown by crosses

Figure 9 shows a scatter plot the resulting goodness of fit values for different simulation traces corresponding to different car densities. Except for the cluster of traces at the very right side with goodness of fit values between 0.6 and 0.65, the exponential distribution shows a tendency of better fit for increasing car densities. The outlier cluster on the right-hand side is actually for a 2-lane scenario, in which the comparably high density and fewer lanes lead to more clustering of cars on the road.

The causes of the deviations of the empiric pdf in Figure 8 will require further analysis. Also, a cdf based goodness of fit metric may not be the best choice due to the deviations caused by the small samples. Nevertheless, it allows identifying first trends of influential parameters as observed in Figure 9. More investigations are planned in future work.

7. MOBILITY WITH DEPENDENCIES BETWEEN VEHICLES

Vehicular ad-hoc networks have received increasing interest in the last years for their potential to support a variety of services and applications in order to improve driving safety or traffic efficiency and to provide information and entertainment to the users. Connectivity between cars in freeway scenarios thereby influences the reliability and quality of the communication applications. Most of the existing connectivity analysis focuses on static snapshots of the geographic mobility. This paper investigates the stochastic process of encountering new nodes in communication range, focusing to a large extend on single-hop (direct link-layer) connectivity.

It is rigorously proven that under certain assumptions the process of encountering new nodes in connectivity range is a *Poisson* process whose rates can be calculated from the car density and the average relative speed. Subsequently, simulation experiments with more complex freeway mobility models are used to check the sensitivity of this result to the underlying assumptions. It thereby shows that the *Poisson* assumption is a good approximation in also more general scenarios of independent car movements, even in multi-hop connectivity situations. The distribution of the connectivity times can also be computed. The influence of the communication radius R on the encounter rate and the mean duration of the connectivity period is derived. Finally, trace driven simulations of a complex freeway mobility simulation from [12] are investigated and the initial analysis results show that an inhomogeneous *Poisson* process whose rate is calculated from the previous established relations presents a good approximation in certain scenarios.

More detailed investigations of mobility models with correlated movements as well as a mathematical treatment of simple multi-hop cases is planned as future extension of this work.

ACKNOWLEDGMENT

Part of this research was supported by the European FP6 project 'Highly DEpendable ip-based NETworks and Services' (www.hidenets.aau.dk), and by the Danish Natural Science Research Council (grant 272-06-0442, "Point Process Modeling and Statistical Inference"). The authors would like to thank the consortium partners for the inspiring discussions and comments. The Telecommunications Research Center Vienna (ftw) is supported by the Austrian Government and by the City of Vienna within the competence center program COMET.

REFERENCES

- [1] HIDENETs, "Highly dependable ip-based networks and services," <http://www.hidenets.aau.dk/>, IST-FP6-STREP-26979," 2006.
- [2] M. B. Hansen, J. G. Rasmussen, and H.-P. Schwefel, "Connectivity analysis of onedimensional ad-hoc networks," DMF-2008-06-003, 2008.
- [3] HIDENETs, "Highly dependable ip-based networks and services, experimental proof-of-concept set-up hidenets," Project Deliverable D6.3, IST-FP6-STREP-26979, August 2008.
- [4] F. Khadar and D. Simplot-Ryl, "Connectivity and topology control in wireless ad hoc networks with realistic physical layer," Conference on Wireless and Mobile Communications (ICWMC'07), IEEE Computer Society Washington, DC, USA (Proceedings of the Third International), pp. 49, 2007.
- [5] D. Miorandi and E. Altman, "Connectivity in one-dimensional ad-hoc networks: A queueing theoretical approach.," Wireless Networks 12, 573587, 2006.
- [6] Y. Cheng and T. G. Robertazzi, "Critical connectivity phenomena in multihop radio models," IEEE Transactions on Communications, vol. 37(7), 770777, 1989.
- [7] T. Spyropoulos, A. Jindal, and K. Psounis, "An Analytical Study of Fundamental Mobility Properties for Encounter-based Protocols," International Journal of Autonomous and Adaptive Communications Systems, vol. 1, N^o. 1, pp. 4-40, 2008.
- [8] HIDENETs, "Highly Dependable ip-based networks and services, use case scenarios and preliminary reference model," in Project Deliverable D1.1, IST-FP6-STREP-26979, Sept. 2006.
- [9] C2CCC, "Car 2 car communication consortium manifesto, overview of the c2c-cc system," version 1.1, august, 2007, http://www.car-tocar.org/fileadmin/downloads/C2C_CC_manifesto_v1.1.pdf.
- [10] J. Møller and R. P. Waagepetersen, "Statistical Inference and Simulation for Spatial Point Processes," Chapman & Hall, Boca Raton, Florida, 2004.
- [11] E. Matthiesen Moller, O. Hamouda, M. Kaâniche, and S. H.-P., "Dependability evaluation of a replication service for mobile applications in dynamic ad-hoc networks," ISAS08, Tokyo, Japan (Lecture Notes in Computer Science 5017 Springer'08), pp. 171-186, 2008.
- [12] H. F. Bler, M. Torrent-Moreno, R. Krüger, M. Transier, H. Hartenstein, and W. Effelsberg, "Studying vehicle movements on highways and their impact on ad-hoc connectivity," Technical report, University of Mannheim, department for mathematics and computer science, June 2005.